Supporting Information

Highly crystalline sodium manganese ferrocyanide microcubes for advanced sodium ion battery cathodes

Fangwei Peng,[a] Lei Yu,[b] Pengyue Gao,[c,d] Xiao-Zhen Liao,*[a] Jianguo Wen,[b] Yushi He,[a] Guoqiang Tan,[e] Yang Ren,[c] and Zi-Feng Ma[a]

a. Shanghai Electrochemical Energy Devices Research Center, Department of Chemistry and Chemical Engineering, Shanghai Jiao Tong University, Shanghai 200240, China.
E-mail: liaoxz@sjtu.edu.cn;

b. Center for Nanoscale Materials, Argonne National Laboratory, Argonne, IL 60439, USA.

c. X-ray Science Division, Argonne National Laboratory, IL 60439, USA.

d. State Key Laboratory of Advanced Special Steel & Shanghai Key Laboratory of Advanced Ferrometallurgy & School of Materials Science and Engineering, Shanghai University, Shanghai 200072, China.

e. School of Materials Science & Engineering, Beijing Institute of Technology, Beijing 100081, China.

Table S1 ICP results of the as-prepared PBM samples (Fe/Mn/Na molar ratio)

Samples	Fe	Mn	Na	Chemical formula
H-PBM	0.98	1	1.95	$Na_{1.92}Mn[Fe(CN)_6]_{0.98}\square_{0.02}$
L-PBM	0.90	1	1.62	$Na_{1.60}Mn[Fe(CN)_6]_{0.9}\square_{0.10}$

In this work, the synthesis process of Na2MnFe(CN)6 microcubes (H-PBM) was in room temperature. In this condition the [Fe(CN)6]4- could not decompose to generate Fe2+ and CN- , thus the number of (CN)6 was directly related to Fe content . Actually self-decomposition of [Fe(CN)6]4- only occurs in hot acidic solution. In the preparation of L-PBM no acidic reagent was used, thus the chemical composition of obtained NaxMn[Fe(CN)6]y both for H-PBM and L-PBM can be calculated from ICP results of Na/Mn/Fe. As shown in Table S1 the ICP results of Fe/Mn/Na were 0.98/1/1.95 for H-PBM and 0.90/1/1.62 for L-PBM respectively in this work. Considering the charge balance we described the chemical formula of H-PBM as Na1.92Mn[Fe(CN)6]0.98□0.02 (□ represents a [Fe(CN)6]4- vacancy), and chemical formula of L-PBM as Na1.60Mn[Fe(CN)6]0.9□0.10.

Table S2. The comparison of representative Prussian blue analogue materials for sodium-ion batteries.

Composition Synthesis method	Size (μm)	Reversible capacity in Na cells (mAh g^{-1} / mA g^{-1})	Average working voltage (V vs. Na^+/Na)	Rate Performance (mAh g^{-1})	Cycle life
$Na_{0.84}Ni[Fe(CN)_6]_{0.71}\cdot 6H_2O$[1] Simple co-precipitation	~0.05	66 / 20	3.1	N.A.	99.7%@200th at 20 mA g^{-1}
$Na_2Zn_3[Fe(CN)_6]_2\cdot xH_2O$[2] Simple co-precipitation	~0.5	56.4 / 10	3.3	N.A.	85.2%@50th at 10 mA g^{-1}
$Na_{0.7}Ti[Fe(CN)_6]_{0.9}$[3] Simple co-precipitation	0.1-0.15	92.3 / 50	3.4/3.0	38 mAh g^{-1} / 4C	70%@50th at 50 mA g^{-1}
$Cu_3[Fe(CN)_6]_2$[4] Simple co-precipitation	0.03-0.08	44 / 20	3.3	25 mAh g^{-1} / 1C	57.1%@50th at 20 mA g^{-1}
$FeFe(CN)_6$[5] Simple co-precipitation	~0.4	120 / 60	3.4/2.8	78 mAh g^{-1} / 20C	87%@500th at 2 C
$Na_{0.61}Fe[Fe(CN)_6]_{0.94}\cdot 2.79H_2O$[6] Acid-assisted single iron-source	0.3-0.6	170 / 25	3.4/2.7	70 mAh g^{-1} / 4C	100%@150th at 0.2 C
$Na_{1.56}FeFe(CN)_6\cdot 3.1H_2O$[7] Acid-assisted single iron-source	0.5-3	103.6 / 20	3.4/2.9	90 mAh g^{-1} / 1C	97%@400th at 20 mA g^{-1}
$Na_{1.63}Fe[Fe(CN)_6]_{0.89}$[8] Acid-assisted single iron-source	1-3	150 / 25	3.5/2.6	N.A.	90%@200th at 25 mA g^{-1}
$Na_{1.70}FeFe(CN)_6$[9] Citrate as chelating agent	~0.05	129 / 200	3.45/2.7	71.2 mAh g^{-1} / 12C	70.5%@100th at 200 mA g^{-1}
$Na_{1.73}Fe[Fe(CN)_6]_{0.98}$[10] Simple co-precipitation	0.06-0.1	123 / 100	3.25/ 2.85	78 mAh g^{-1} / 8C	73%@200th at 1 C
Dehydrated $Na_{1.92}FeFe(CN)_6$[11] Acid-assisted single iron-source	0.8-4	160 / 10	3.29/3.0	145 mAh g^{-1} / 10C	80%@750th at 2 C
$Na_{1.95}Fe[Fe(CN)_6]_{0.93}\cdot \square_{0.07}$[12] Citrate as chelating agent	3-4	~120 / 50	3.02/ 2.87	60 mAh g^{-1} / 16C	79%@280th at 100 mA g^{-1}
$Na_{1.60}Co[Fe(CN)_6]_{0.90}\cdot 2.9H_2O$[13] Electrochemical deposition	N.A.	139 / 70	3.8/3.4	121 mAh g^{-1} / 60C	71%@100th at 0.6 C
$Na_{1.85}Co[Fe(CN)_6]_{0.99}\cdot 1.9H_2O$[14] Citrate as chelating agent	~0.6	153 / 10	3.8/3.2	60 mAh g^{-1} / 5C	90%@200th at 200 mA g^{-1}
$Na_{1.32}Mn[Fe(CN)_6]_{0.83}\cdot 3.5H_2O$[15] Electrochemical deposition	~1	109 / 50	3.6/3.2	80 mAh g^{-1} / 20C	90%@100th at 0.5 C
$Na_{1.72}Mn[Fe(CN)_6]_{0.99}\cdot 2.0H_2O$[16] Simple co-precipitation	N.A.	134 / 6	3.57/ 3.27	46 mAh g^{-1} / 40C	90%@30th at 6 mA g^{-1}
R-$Na_{1.89}Mn[Fe(CN)_6]_{0.97}$[17] Simple co-precipitation (in 25% ethanol solution)	0.08-0.35	150 / 15	3.44	121 mAh g^{-1} / 20C	75%@500th at 100 mA g^{-1}
$Na_{1.96}Mn[Mn(CN)_6]_{0.99}\cdot 2H_2O$[18]	~0.1	209 / 40	3.6/2.8	156 mAh g^{-1}	75%@100th

Simple co-precipitation				/ 5C	at 2 C
$Na_{1.7}MnFe(CN)_6 \cdot 2.38H_2O$[19] Citrate as chelating agent	0.2-0.5	136.8 / 12	3.45/ 3.25	~10 mAh g^{-1} / 40C	~45%@200th at 2 C
$Na_{1.92}Mn[Fe(CN)_6]_{0.98} \cdot 1.38H_2O$ dissociation/precipitation method using EDTA-$MnNa_2$ precursor (in this work)	3-5	152.8 / 10	3.45	110.3mAh g^{-1} / 10C	82%@500th at 100 mA g^{-1}

References:

1 Y. You, X. Wu, Y. Yin and Y. Guo, *J MATER CHEM A*, 2013, **1**, 14061.

2 H. Lee, Y. Kim, J. Park and J. W. Choi, *CHEM COMMUN*, 2012, **48**, 8416.

3 M. Xie, Y. Huang, M. Xu, R. Chen, X. Zhang, L. Li and F. Wu, *J POWER SOURCES*, 2016, **302**, 7-12.

4 S. Jiao, J. Tuo, H. Xie, Z. Cai, S. Wang and J. Zhu, *MATER RES BULL*, 2017, **86**, 194-200.

5 X. Wu, W. Deng, J. Qian, Y. Cao, X. Ai and H. Yang, *J MATER CHEM A*, 2013, **1**, 10130.

6 Y. You, X. Wu, Y. Yin and Y. Guo, *Energy Environ. Sci.*, 2014, **7**, 1643-1647.

7 W. Li, S. Chou, J. Wang, Y. Kang, J. Wang, Y. Liu, Q. Gu, H. Liu and S. Dou, *CHEM MATER*, 2015, **27**, 1997-2003.

8 Y. You, X. Yu, Y. Yin, K. Nam and Y. Guo, *NANO RES*, 2015, **8**, 117-128.

9 Y. Liu, Y. Qiao, W. Zhang, Z. Li, X. Ji, L. Miao, L. Yuan, X. Hu and Y. Huang, *NANO ENERGY*, 2015, **12**, 386-393.

10 Y. Yang, E. Liu, X. Yan, C. Ma, W. Wen, X. Liao and Z. Ma, *J ELECTROCHEM SOC*, 2016, **163**, A2117-A2123.

11 L. Wang, J. Song, R. Qiao, L. A. Wray, M. A. Hossain, Y. Chuang, W. Yang, Y. Lu, D. Evans, J. Lee, S. Vail, X. Zhao, M. Nishijima, S. Kakimoto and J. B. Goodenough, *J AM CHEM SOC*, 2015, **137**, 2548-2554.

12 Y. Huang, M. Xie, J. Zhang, Z. Wang, Y. Jiang, G. Xiao, S. Li, L. Li, F. Wu and R. Chen, *NANO ENERGY*, 2017, **39**, 273-283.

13 M. Takachi, T. Matsuda and Y. Moritomo, *APPL PHYS EXPRESS*, 2013, **6**.

14 X. Wu, C. Wu, C. Wei, L. Hu, J. Qian, Y. Cao, X. Ai, J. Wang and H. Yang, *ACS APPL MATER INTER*, 2016, **8**, 5393-5399.

15 T. Matsuda, M. Takachi and Y. Moritomo, *Chemical communications (Cambridge, England)*, 2013, **49**, 275-2752.

16 L. Wang, Y. Lu, J. Liu, M. Xu, J. Cheng, D. Zhang and J. B. Goodenough, *Angewandte Chemie International Edition*, 2013, **52**, 1964-1967.

17 J. Song, L. Wang, Y. Lu, J. Liu, B. Guo, P. Xiao, J. Lee, X. Yang, G. Henkelman and J. B. Goodenough, *J AM CHEM SOC*, 2015, **137**, 2658-2664.

18 H. Lee, R. Y. Wang, M. Pasta, S. Woo Lee, N. Liu and Y. Cui, *NAT COMMUN*, 2014, **5**.

19 W. Li, S. Chou, J. Wang, J. Wang, Q. Gu, H. Liu and S. Dou, *NANO ENERGY*, 2015, **13**, 200-207.

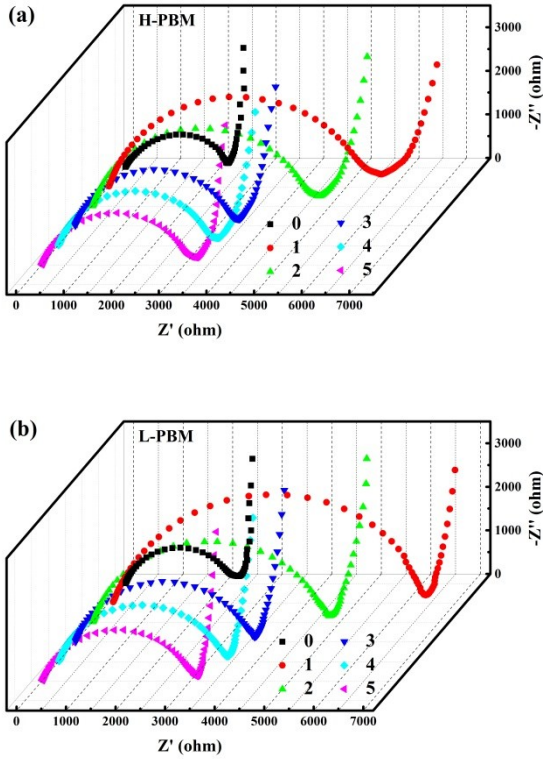

Fig. S1 EIS plots of (a) H-PBM and (b) L-PBM cells before cycle and after 1st , 2nd, 3rd, 4thand 5th cycle at 0.1C rate, respectively.

The EIS plots of H-PBM and L-PBM cells were recorded before cycle and after 1st, 2nd, 3rd, 4th and 5th cycle at 0.1C rate, respectively. It is clear that all the EIS plots consist one depressed semicircle in the high frequency region and an inclined line in the low frequency region. The depressed semicircle at higher frequency region represents the impedance of charge transfer process. The slop at low frequency region reflects a semi-infinite Warburg diffusion process. It can be seen that after the first cycle, the charge transfer resistance obviously increased owing to the formation of SEI on the electrode surface. Then the resistance decreased in the subsequent cycles as the SEI film turn to be stable. It is noted that even though the larger surface area of L-PBM may benefit the interface charge transfer reaction the observed electrochemical impedance of the L-PBM electrode was still similar or slightly larger than that of the H-PBM electrode for each tested cycle. This result indicates that the enhanced Na^+ transfer kinetic of H-PBM ensured its good electrochemical performance in spite of its large particle size.

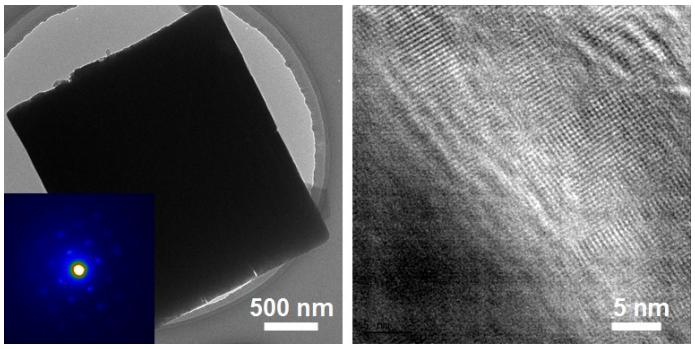

Fig. S2 TEM, HRTEM images and selected area electron diffraction (SAED) pattern of a H-PBM particle after 500 cycles.